EARTH SURFACE PROCESSES AND LANDFORMS
Earth Surf. Process. Landforms **39**, 865–876 (2014)
Published in 2013. This article is a U.S. Government work and is in the public domain in the USA.
Published online 12 November 2013 in Wiley Online Library
(wileyonlinelibrary.com) DOI: 10.1002/esp.3488

Post-fire bedload sediment delivery across spatial scales in the interior western United States

Joseph W. Wagenbrenner[1,2†*] and Peter R. Robichaud[2]
[1] Department of Biological Systems Engineering, Washington State University, Pullman, WA USA
[2] US Department of Agriculture, Forest Service, Rocky Mountain Research Station, Moscow, ID USA

Received 22 March 2013; Revised 18 September 2013; Accepted 26 September 2013

*Correspondence to: Joseph W. Wagenbrenner, School of Forest Resources and Environmental Science, Michigan Technological University, 1400 Townsend Drive, Houghton, MI, 49931-1295, USA. E-mail: jwwagenb@mtu.edu
†Current affiliation: School of Forest Resources and Environmental Science, Michigan Technological University, Houghton, MI USA

ESPL
Earth Surface Processes and Landforms

ABSTRACT: Post-fire sediment yields can be up to three orders of magnitude greater than sediment yields in unburned forests. Much of the research on post-fire erosion rates has been at small scales (100 m^2 or less), and post-fire sediment delivery rates across spatial scales have not been quantified in detail. We developed relationships for post-fire bedload sediment delivery rates for spatial scales up to 117 ha using sediment yield data from six published studies and two recently established study sites. Sediment yields and sediment delivery ratios (SDRs; sediment delivered at the catchment scale divided by the sediment delivered from a plot nested within the catchment) were related to site factors including rainfall characteristics, area, length, and ground cover. Unit-area sediment yields significantly decreased with increasing area in five of the six sites. The annual SDRs ranged from 0.0089 to 1.15 and these were more closely related to the ratio of the plot lengths than the ratio of plot areas. The developed statistical relationships will help quantify post-fire sediment delivery rates across spatial scales in the interior western United States and develop process-based scaling relationships. Published in 2013. This article is a U.S. Government work and is in the public domain in the USA.

KEYWORDS: erosion; hillslope; catchment; sedimentation; rainfall intensity

Introduction

Hillslope erosion rates after forest fires can increase dramatically (Swanson, 1981; DeBano *et al.*, 1998; Shakesby and Doerr, 2006; Moody and Martin, 2009) because of temporary changes to hydrologic properties (Robichaud, 2000; Martin and Moody, 2001; Larsen *et al.*, 2009; Ebel *et al.*, 2012). There is evidence that these erosion rates depend on the severity of the wildfire (Robichaud, 2000; Benavides-Solorio and MacDonald, 2001, 2005; Moody *et al.*, 2008b), the magnitude or intensity of the rainfall that occurs after the fire (Moody and Martin, 2001b, 2009; Robichaud *et al.*, 2008b; Lanini *et al.*, 2009), and the geomorphic setting of the burned area (Moody *et al.*, 2008a; Robichaud *et al.*, 2013b).

Much of the research into the hydrologic and geomorphic effects of wildfires has occurred at spatial extents of 100 m^2 or less. A few observational studies have recorded elevated sediment yields at larger (e.g. > 1 km^2) scales (Rowe *et al.*, 1954; Brown, 1972; Helvey, 1980; Meyer *et al.*, 1992; Troendle and Bevenger, 1996; Moody and Martin, 2001a; Lane *et al.*, 2006; Malmon *et al.*, 2007; Reneau *et al.*, 2007; Noske *et al.*, 2010). However there are relatively few studies relating the post-fire sediment response across spatial scales (Ferreira *et al.*, 2008; Mayor *et al.*, 2011).

Sediment delivery across scales has been a focus in the hydrologic and geomorphic literature for the past several decades (Walling, 1983). It is clear that there is no simple ratio applicable across locations, spatial scales, or land cover type (e.g. forest, range, or grassland) or condition, and that the sediment delivery rate relative to the hillslope erosion rate is a complex, dynamic, approximate concept (Walling, 1983; de Vente and Poesen, 2005; Parsons *et al.*, 2006b; de Vente *et al.*, 2007). Still, there is much practical value in determining an approximate proportion of the delivery of eroded sediment to points downstream (Lu *et al.*, 2005; Parsons *et al.*, 2006a).

Given the impacts of forest fires on storm flows and erosion rates, the sediment delivery issue is of great concern to those trying to manage downstream resources. In the United States and increasingly in other countries, post-fire assessments attempt to predict the risk of sedimentation, among other issues, in streams and reservoirs below burned areas. Often the best information available to these managers is an erosion rate measured at a relatively small spatial scale, and there is little guidance on the error associated with extrapolating these small-scale erosion rates to basin scale sediment yields. Physically-based erosion models may help address the difference in sediment delivery across spatial scales but models should be validated at each scale of inference, and few data

are available on post-fire sediment delivery rates at spatial scales greater than about 20 ha.

Controls on post-fire sediment yields at the hillslope scale have been fairly well described, and include amount of ground cover (Vega and Diaz-Fierros, 1987; Prosser and Williams, 1998; Robichaud, 2000; Benavides-Solorio and MacDonald, 2001, 2005; Cerdà and Doerr, 2005; Doerr *et al.*, 2006; Wagenbrenner *et al.*, 2006; Larsen *et al.*, 2009); the degree of heating of the soil, usually inferred after the fire by assessing soil burn severity (Keeley, 2009); the observed post-fire rainfall amount or intensity (Vega and Diaz-Fierros, 1987; Moody and Martin, 2001b, 2009; Wondzell and King, 2003; Kunze and Stednick, 2006; Desilets *et al.*, 2007; Spigel and Robichaud, 2007; Robichaud *et al.*, 2008b); hillslope shape (planar, convex, or concave) (Benavides-Solorio and MacDonald, 2005); and time since burning (Morris and Moses, 1987; Benavides-Solorio and MacDonald, 2005; Wagenbrenner *et al.*, 2006; Robichaud *et al.*, 2008b, 2013b, 2013c; Larsen *et al.*, 2009; Pierson *et al.*, 2009).

Some progress has been made in establishing scaling relationships in burned areas. Channel network patterns were characterized and related across three spatial scales (1 to 1000 m^2, 0.1 to 100 ha, and 1 to 1000 km^2) in a study three years after the Buffalo Creek fire in Colorado (Moody and Kinner, 2006). The authors concluded that the scaling ratios in the largest size class (1 to 1000 km^2) applied to the middle size class (0.1 to 100 ha), but the rill networks in the smallest size class (1 to 1000 m^2) produced a less-dense channel network than predicted by scaling from the two larger classes (Moody and Kinner, 2006).

The goal of the current study was to use field-measured sediment yields from fluvial events to determine how post-fire sediment delivery rates vary across spatial scales. The specific objectives were to: (1) develop an empirical relationship between sediment yields, spatial extent, and site and rainfall characteristics; (2) determine if this relationship holds across multiple locations in the interior western United States with diverse climate and topography; (3) calculate the post-fire sediment delivery ratio (*SDR*) across spatial scales and relate this to physical properties.

Methods

Site description

Study sites were installed after wildfires in six forests in Colorado, Washington, Utah, Montana, and Arizona (Figure 1). Detailed site descriptions and methods are presented in previous studies for four of the sites: Bobcat in north central Colorado (Wagenbrenner *et al.*, 2006); Hayman in central Colorado (Robichaud *et al.*, 2008b, 2013b, 2013c); North 25 in north-central Washington (Robichaud *et al.*, 2006, 2008b) and Valley in south western Montana (Robichaud *et al.*, 2008a, 2008b). The methods at the Twitchell site in Utah and the Wallow site in Arizona (Figure 1) followed the methods used in the earlier studies and these are briefly summarized later along with the earlier sites' descriptions (Tables I and II). All of the sites used sediment traps to retain sediment delivered from plots or catchments at multiple spatial scales. In cases when the runoff quantity was less than the trap storage capacity, the measured sediment delivery was the total load. Generally, though, the majority of the runoff volumes exceeded the storage capacity of the traps and so the sediment measurements were the bedload fraction.

The Twitchell site was located within the 180 km^2 Twitchell Canyon fire of July 2010 on the Fishlake National Forest in Utah. This was the only site that was not a mixed-conifer forest before the fire, and its vegetation was composed of pinyon pine, juniper,

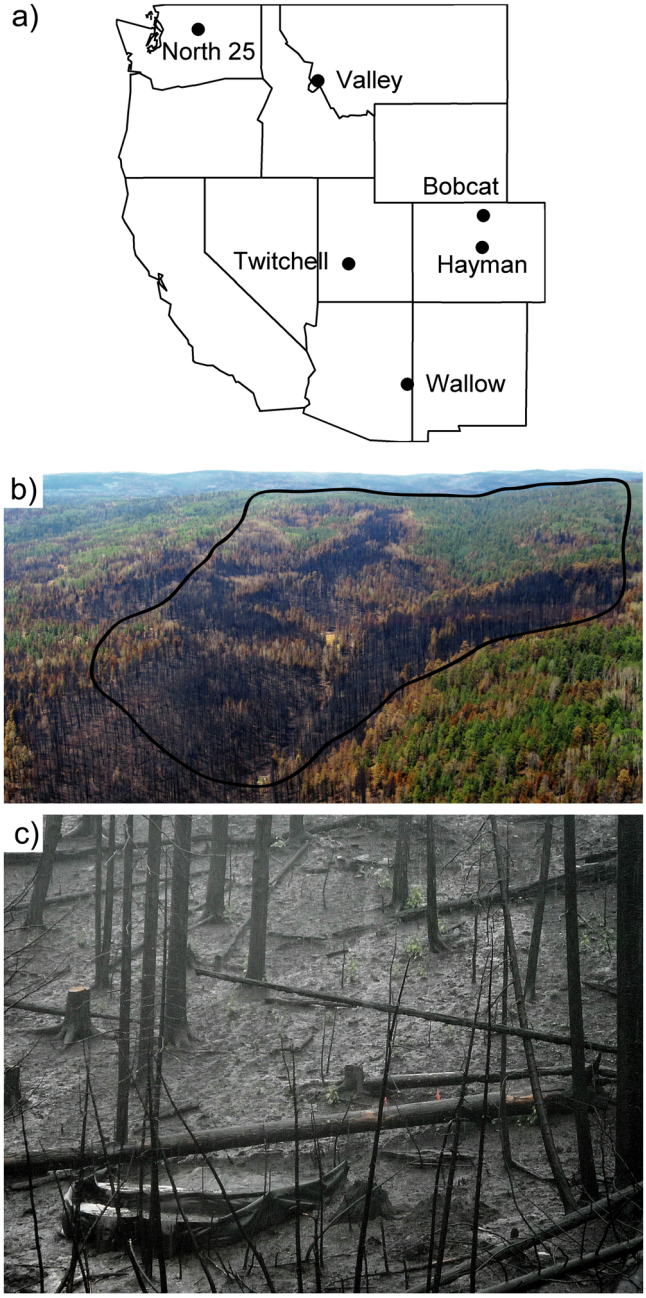

Figure 1. (a) Locations of the six study sites in the western US. (b) Oblique view looking up the West Willow Creek drainage at the Wallow site on 30 June 2011; outline shows approximate catchment boundary. (c) Hillslope plot and silt fence at the Wallow site during a runoff event 10 August 2011. This figure is available in colour online at wileyonlinelibrary.com/journal/espl

and Gambel oak (*Pinus edulis*, *Juniperus scopulorum*, and *Quercus gambelii*, respectively) (Table I). The five catchments were the control catchments (0.22 to 1.6 ha) that had been paired with five catchments treated with straw bale check dams in a larger study to measure the effect of the check dams on sediment yields (Storrar, 2013). Nested hillslope plots were installed in the headwaters of four of these untreated catchments. Five additional hillslope plots were installed upstream of the check dams in the treated catchments, and these were included in the current study without the corresponding catchment-scale data. The nine plots were 3 m wide by 9 to 63 m long along the slope, and had gradients between 25% and 67% (Table III). Rain gages were installed in or adjacent to each catchment and the nearest gage was used to characterize rainfall for each plot.

The Wallow site was located in the 117 ha West Willow Creek catchment, which burned in June 2011 during the

Table I. Fire year, years of data and post-fire years used in the study, latitude, longitude, elevation, and dominant pre-fire vegetation for each site

Site	Fire year	Data years	Post-fire years	Latitude (deg)	Longitude (deg)	Elevation (m)	Pre-fire vegetation [b]
Bobcat[c]	2000	2000–2002	0–2[a]	40.45	–105.35	2300	Mixed: ponderosa pine (*Pinus ponderosa*)
Hayman[d]	2002	2002–2004	0–2[a]	39.18	–105.36	2400	Mixed: ponderosa pine (*Pinus ponderosa*)
North 25[e]	1998	1999–2000	1–2	47.99	–120.34	1600	Mixed: grand fir (*Abies grandis*)
Twitchell[f]	2010	2011–2012	1–2	38.53	–112.40	2200	Twoneedle pinyon pine, Rocky Mountain juniper, Gambel oak (*Pinus edulis, Juniperus scopulorum, Quercus gambelii*)
Valley[g]	2000	2001–2002	1–2	45.91	–114.03	1700	Mixed: Douglas-fir (*Pseudotsuga menziesii*)
Wallow[h]	2011	2011–2012	0–1[a]	33.66	–109.31	2600	Mixed: Douglas-fir (*Pseudotsuga menziesii*)

[a]Post-fire year 0 (the fire year) is from the time the fire occurred until the end of the following snowmelt.
[b]'Mixed' indicates mixed conifer forest. In these cases the dominant tree types are indicated.
[c]Wagenbrenner *et al.*, 2006
[d]Robichaud *et al.*, 2008b; 2013b; 2013c
[e]Robichaud *et al.*, 2008b; 2006
[f]Storrar, 2013
[g]Robichaud *et al.*, 2008a; 2008b
[h]Wagenbrenner, 2013

Table II. Dominant soil classification(s), soil texture, geologic parent material, 2-yr return interval and observed minimum (Min) and maximum (Max) 10-min maximum rainfall intensity (I_{10}), and number of plot-events (n) for each site

Site	Soil classification	Soiltexture	Parent material	I_{10} (mm hr^{-1}) 2-yr	I_{10} (mm hr^{-1}) Min–Max	*n*	Reference(s)
Bobcat	Lamellic Haplucryepts Ustic Dystrocryepts Typic Haplustolls Lithic Haplustalfs	Gravelly sandy loam	Schist, gneiss	52 [a]	6–55	102	Wagenbrenner *et al.*, 2006
Hayman	Typic Ustorthents Typic Cryorthents	Gravelly sandy loam	Granitic	56 [a,b]	6–75	82	Robichaud *et al.*, 2008b; 2013b, 2013c
North 25	Typic Vitrixerands	Ashy sandy loam	Volcanic	32 [a]	3–31	35	Robichaud *et al.*, 2006; 2008b
Twitchell	Aridic Argiustolls Aridic or Typic Haplustolls	Gravelly loam	Volcanic tuff and rhyolite	48 [c]	11–61	119	Storrar, 2013
Valley	Typic Haplustepts	Gravelly sandy loam	Grantic colluvium	31 [a]	7–59	29	Robichaud *et al.*, 2008a,2008b
Wallow	Typic Hapludalfs Typic Haplocryalfs Lithic or Pachic Argiustolls Typic Haplustalfs	Silty clay loam	Basalt	81 [c]	9–47	124	USDA Forest Service, 2011a

[a]Miller *et al.*, 1973
[b]Arkell and Richards, 1986
[c]Bonnin *et al.*, 2004

2200 km^2 Wallow fire on the Apache-Sitgreaves National Forest in Arizona (Figure 1). A concrete weir was installed in West Willow Creek in 1962 as part of an earlier study (Heede, 1985). In July 2011 the weir was re-instrumented and the stilling ponds were emptied and surveyed. Four slope-length plots were installed near the weir, and these were between 130 and 322 m long (Table III). Twelve 12-m long burned, untreated plots were installed as control plots for a study on the effectiveness of post-fire seeding, and these were bounded by trenches to exclude flow from above the plots. The width of each plot was 3 m. Mean slope gradients ranged from 30 to 36% for the hillslope plots (Table III). Four rain gages were installed throughout the catchment. The nearest gage was used to characterize rainfall for the hillslope plots and the median of the four rain gage values was used to characterize the rainfall for the catchment. Sediment delivered at the catchment scale was attributed to runoff events recorded by a stream gaging station, and in at least one case the spring freshet produced sediment at the catchment scale with no corresponding sediment delivered at the hillslope scales. Additional site details, including the stream gaging station, are described in a study on post-fire runoff rates (Wagenbrenner, 2013).

In order to assess the relative importance of rainfall and site characteristics at different spatial scales, each plot and catchment was categorized by its contributing area into one of four classes. These classes were defined by breaks among plot or catchment areas so that plots or catchments with similar areas fell into the same area class. Breaks between area classes were: 80 m^2, 0.1 ha, and 10 ha (Table III). The smallest two classes (area < 80 m^2 and 80 m^2 $<$ area $<$ 1000 m^2) were non-convergent plots (< 80 m^2) or hillslopes (80 m^2 to 1000 m^2) and each site included at least one of these area classes (Table III). The two

Table III. Total number of plots (*N*), the number of plots or catchments (*n*) in each area class (Class), and the minimum and maximum slope and length for each area class by site

		Class 1: 20–80 m^2			Class 2: 80–1000 m^2			Class 3: 0.1 ha–10 ha			Class 4: > 10 ha		
		(non-convergent)			(non-convergent)			(convergent, channelized)			(convergent, channelized)		
Site	*N*	*n*	Slope (%)	Length (m)	*n*	Slope (%)	Length (m)	*n*	Slope (%)	Length (m)	*n*	Slope (%)	Length (m)
Bobcat	12	0			3	28–37	22–48	9[b]	24–60	60–212	0		
Hayman	10	8	19–44	7–14	0			2	31–33	429–452	0		
North 25	9	8[a]	28–54	8–9	0			0			1	50	537
Twitchell	14	5[a]	39–67	9–19	4[a]	25–62	37–64	5	38–57	115–188	0		
Valley	5	0			4	52–61	17–18	1	46	285			
Wallow	15	10[a]	30–36	11–13	4[a]	30–36	129–321	0			1	6.8	1297

[a]These sites had plots nested within catchment(s) which were used in sediment delivery ratio (*SDR*) calculations and analysis: two Class 1 plots at North 25; two Class 1 and two Class 2 plots at Twitchell; and six Class 1 and four Class 2 plots at Wallow.
[b]None of the Bobcat plots had defined channels.

larger classes (0.1 ha < area < 10 ha and area >10 ha) were convergent hillslopes or catchments and each site also included at least one of these larger classes (Table III). Well-defined channels were present in the catchments in the two largest classes, except for the plots in the 0.1 ha to 10 ha class at the Bobcat site.

According to the Wallow fire burn severity map (USDA Forest Service, 2011b) which was derived from differenced normalized burn ratios, the Wallow catchment was unique in that it was only partly (~50%) burned at high severity, with an additional 20% of the area burned at low or moderate severity and about 30% of the catchment unburned. The mapped burn severity classification was verified along three transects in or near the West Willow Creek catchment using field measurements and observations (Parsons *et al.*, 2010). All of the unburned areas and the areas burned at low or moderate severity were in the upper parts of the catchment (Wagenbrenner, 2013). While this pattern is typical in wildfires in this area (e.g. Haire and McGarigal, 2010), these lesser-impacted areas would contribute little or no sediment as compared to the sediment produced from the areas burned at high severity (Benavides-Solorio and MacDonald, 2005). As we did not measure the contribution of each burn class separately, we assumed the whole catchment contributed to the sediment delivery at the outlet. This conservative approach allowed us to analyze the catchment-scale sediment delivery as impacted by the representative heterogeneous burn severity found in this region. All of the other plots and catchments burned at high severity. The Wallow catchment also historically had runoff through most of the year (Heede, 1985) whereas all the other plots and catchments were ephemeral.

Sediment yields in the smallest plots were measured using silt fences (Robichaud and Brown, 2002). The sediment yields in the catchments were measured using weirs made of wood and geotextile (Twitchell) (Storrar, 2013), galvanized sheet metal (North 25, Valley, and Hayman) (Robichaud, 2005) or concrete (Wallow). The accumulated sediment in the silt fences was weighed on site and subsampled for gravimetric sediment moisture content. Sediment volume in the weirs was calculated from repeat surveys and sampled for bulk density. Dry sediment mass was calculated from the field-measured weights or volumes and the sediment moisture content or bulk density. Sediment yield was the dry sediment mass divided by the planimetric contributing area at the weir or silt fence.

We use the term 'fire year' to represent measurements or observations made in the period between the fire occurrence and the first winter after the fire. 'First post-fire year' commenced in the spring of the calendar year following the fire and 'second post-fire year' began in the subsequent spring. We differentiate 'fire year' from 'first post-fire year' because within the geographic region represented by the study the fire's effects on soils and vegetation are greatest during the period between the wildfire and the first winter (Robichaud *et al.*, 2008b, 2013a). The annual sediment yield in the fire year was the sum of sediment delivered by each plot or catchment between the time of the fire and the end of the following snow melt period (April or May, depending on the site). The annual yields for the first and second post-fire year consisted of the total sediment delivered between the subsequent snow-free date and the end of the following snowmelt period.

Multiple tipping bucket rain gages were located at all sites except North 25, which had just one. Storm events were separated by a six hour period with no rainfall and summarized by the event total rainfall (in millimeters), maximum 10-minute, 30-minute, and 60-minute rainfall intensities (I_{10}, I_{30}, and I_{60}, respectively) (in mm hr^{-1}). Sediment yields at all scales were measured on an event basis as much as feasible, but in several cases the sediment yields spanned multiple rainfall events. For

these events the sum of the rainfall and the maximum rainfall intensity that occurred between site visits was associated with each sediment yield value. Ground cover was measured in late summer or early fall using point-intercept classification methods on transects or quadrats within each study catchment or plot. The ground cover for the catchment at the Wallow site was measured in areas of high burn severity.

Statistical analysis

Linear mixed-effects models with repeated measures on plots or catchments were used to assess differences in non-zero sediment yields and *SDR*s among sites, area classes, and controlling site characteristics (SAS Institute Inc., 2008). The *SDR* was calculated for sites with plots nested within catchments (North 25, Twitchell, and Wallow) (Table III), and was the catchment sediment yield divided by the plot sediment yield. Similarly, the area ratio and length ratio were the ratios of the catchment value to those of the plot.

The serial correlation (covariance) among measurements on a given plot or catchment was modeled as a random effect using a spatial power function on the number of days between the start of the fire and the sediment-producing event (Littell *et al.*, 2006). A second random effect was included in each model for the site. For sediment yields, the post-fire year (year of the fire, first post-fire year, or second post-fire year) was added as a fixed effect. The significance level was 0.05 for all analyses. The sediment yields and *SDR*s were log-transformed prior to statistical analysis to satisfy the assumptions of normality and homoscedasticity of the statistical models' residuals, while the contributing areas and area ratios were log-transformed to allow the statistical software's calculation of the confidence limits of the model's estimates.

Continuous variables including I_{10}, I_{30}, I_{60}, event rainfall, ground cover, mean plot or catchment slope, total plot or catchment relief, and planimetric plot or channel length were tested for significance as covariates in the sediment yield models and included in the models if they were significant (forward selection). None of the variables were controlled. If multiple rainfall characteristics (I_{10}, I_{30}, I_{60}, or event rainfall) were significant, only the characteristic with the greatest *F*-statistic was included in the model (Ott, 1993). Similarly, *F*-values were used to determine relative importance of the fixed effects and covariates in the linear mixed-effects models. Models were run for all sites combined and by site to distinguish specific site responses. Linear relationships between sediment yields and individual covariates were developed using the model coefficients (intercepts for post-fire year and modeled slope terms for continuous variables), the observed data for the specific covariate of interest, and the average values of the observed data for the other significant covariates.

The contributing area classes were used to assess the effects of contributing area and rainfall intensity on sediment yields using a linear mixed-effects model with the same model structure as described earlier. This model related event sediment yields to I_{10} within the area classes described earlier.

The uncertainty in the sediment yield and sediment delivery statistical models was assessed using a coefficient of determination for linear mixed-effects models (Nakagawa and Schielzeth, 2013). This method quantifies the variance in the observed data that is accounted for with the fixed effects ($R^2_{\mathrm{LMM(m)}}$) or fixed and random effects ($R^2_{\mathrm{LMM(c)}}$). We added a modification to $R^2_{\mathrm{LMM(c)}}$ to include the variance explained by the covariates ($R^2_{\mathrm{LMM(cov)}}$).

Only the events that occurred in the first two post-fire years were used for analysis of the sediment yield data for two reasons: few data were available for later post-fire years; and there is some indication that post-fire sediment yields decline considerably after the second post-fire year (Robichaud *et al.*, 2013c).

Results

We observed active rainsplash, sheetwash, and rilling during high-intensity storm events at the Bobcat, Hayman, and Wallow sites. We also observed rills on the hillslopes of the Twitchell site. Channel incision and sediment deposition occurred locally in the established channels in the Hayman, Twitchell, and Wallow catchments.

Factors affecting event sediment yields

Statistical modeling showed the event sediment yields within the first two post-fire years were significantly related to the log-transformed contributing area (log(area)) and also affected by the time since burning (post-fire year), the amount of ground cover, and the rainfall intensity (Table IV). Slope and relief were not significant covariates in the statistical models, and the most significant rainfall intensity measure was I_{10}. The differences among post-fire years were described by the intercepts in the linear models as the slopes for the continuous predictor variables (log(area), ground cover, and I_{10}) did not vary across post-fire years. The intercepts for the fire year and the first post-fire year did not differ from each other or from zero (Table IV), but the intercept for the second post-fire year (−0.38) was lower and this difference was nearly significant ($p = 0.09$). The lower intercept reflects lower sediment yields in the second post-fire year as the sites began to recover (Figure 2).

The modeled slope terms (Table IV) showed the event unit-area sediment yields decreased significantly with increasing area (Figure 2) and ground cover (Figure 3) and increased significantly with increasing event I_{10} (Figure 4). These coefficients were used to develop an exponential relationship between event sediment yield (in Mg ha^{-1}), contributing area (in m^2), and the other significant variables for each post-fire year:

$$\text{Event sediment yield} = k_i \text{Area}^{-0.21} \tag{1}$$

where k_i was the combined coefficient that accounted for the ground cover, I_{10}, and model intercept. The k_i was

$$k_i = 10^{-0.018C_n + 0.042I_i + b_n} \tag{2}$$

where C_n was the ground cover (%) for the n^{th} year; I_i was the I_{10} of the i^{th} event (in mm hr^{-1}); and b_n was the intercept for the n^{th} year (Table IV). Using the mean annual values for ground cover and I_{10}, the k_i values across all sites and events were 3.80 for the year of the fire, 2.98 for the first post-fire year, and 0.838 for the second post-fire year (Figure 2).

The natural variability in the measured data as well as factors that were not included in the statistical models resulted in some scatter of the observed data about the linear mixed-effects models. The fixed effect (post-fire year) explained only 4.3% of the variability in log-transformed sediment yields. The random effects (site and repeated measures on plots within sites) explained another 61%, producing an $R^2_{\mathrm{LMM(c)}}$ of 0.65. When the variability explained by the covariates (ground cover, I_{10}, and log-transformed area) was included, the $R^2_{\mathrm{LMM(cov)}}$ increased to 0.72.

Table IV. Number of plot-events (n) and the linear model intercepts for each post-fire year and the linear model slope terms for the log(area), ground cover, and I_{10}. The 95% confidence intervals for each coefficient are shown in parenthesis

	Fire year		First post-fire year		Second post-fire year		Linear model slope terms		
Site	n	Intercept	n	Intercept	n	Intercept	Log(area)	Ground cover	I_{10}
All sites	87	0.19 (–0.11, 0.50)	238	0.13 (–0.040, 0.30)	166	–0.38 (–0.81, 0.045)	–0.21 (–0.28, –0.14)	–0.018 (–0.023, –0.012)	0.042 (0.036, 0.047)
Bobcat	13	2.2 (1.6, 2.8)	53	2.1 (1.7, 2.5)	36	1.4 (0.24, 2.6)	–0.74 (–1.1, –0.39)	–0.027 (–0.037, –0.017)	0.046 (0.033, 0.060)
Hayman	8	–0.98 (–1.5, –0.44)	27	–1.2 (–1.5, –0.88)	47	–1.5 (–2.3, –0.74)	0.076 (–0.047, 0.20)	0.00045 (–0.011, 0.012)	0.036 (0.026, 0.047)
North 25	0	—[a]	17	1.5 (1.2, 1.7)	18	0.090 (–0.49, 0.67)	–0.35 (–0.52, –0.18)	0.0070 (–0.017, 0.031)	–0.014 (–0.033, 0.0041)
Twitchell	0	—[a]	65	–0.49 (–0.91, –0.077)	54	–1.1 (–2.2, –0.043)	–0.24 (–0.39,–0.085)	0.0074 (–0.0077, 0.022)	0.036 (0.024, 0.049)
Valley	0	—[a]	18	–0.46 (–1.2, 0.31)	11	–0.20 (–1.4, 0.99)	–0.36 (–0.64,–0.090)	–0.045 (–0.089,–0.0017)	0.054 (0.034, 0.074)
Wallow	66	0.51 (0.11, 0.92)	58	0.88 (0.21, 1.5)	0	—[a]	–0.20 (–0.29, –0.12)	–0.031 (–0.043, –0.020)	0.049 (0.035, 0.062)

[a]No data

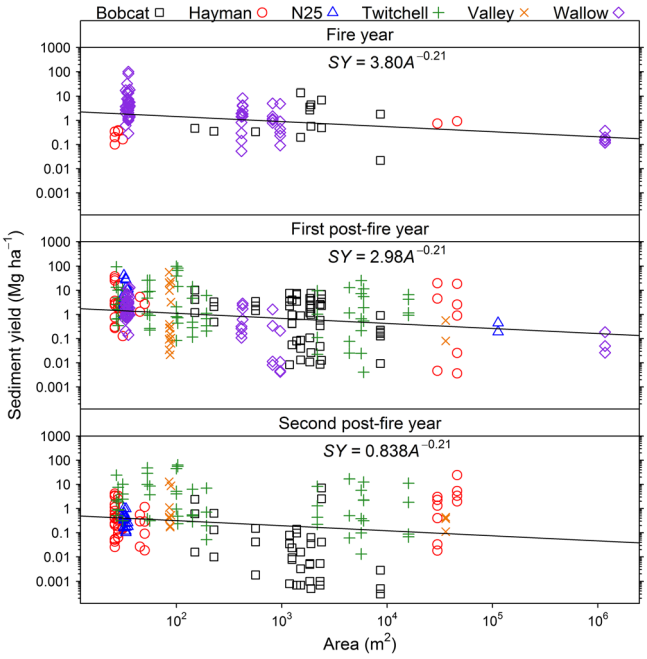

Figure 2. Event sediment yield (SY) versus contributing area (A) by post-fire year. Lines and equations were derived from model coefficients (Table IV; Equations 1 and 2) and average values for ground cover and I_{10} by year. Figure is available in color online.

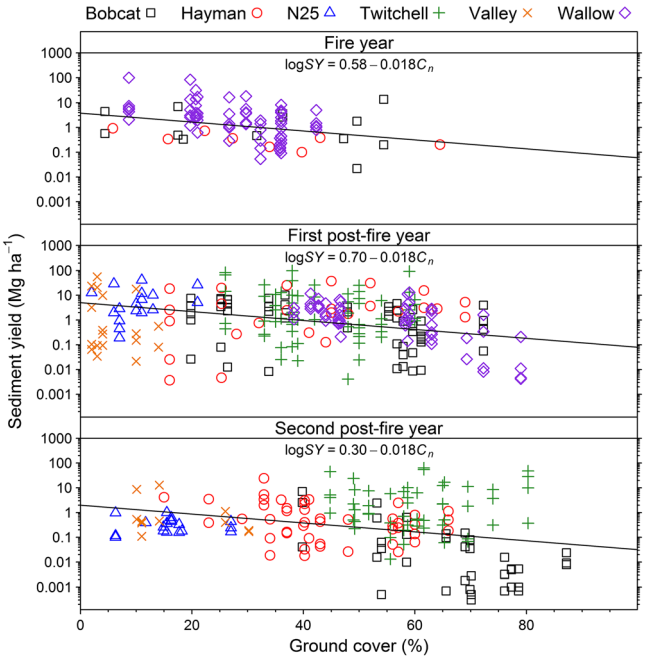

Figure 3. Event sediment yield (SY) versus ground cover (C_n) by post-fire year. Lines and equations were derived from model coefficients (Table IV) and average values for log(area) and I_{10} by year. This figure is available in colour online at wileyonlinelibrary.com/journal/espl

Site differences in factors affecting sediment yields

Some of the modeled slope terms differed across sites (Table IV). The slope for log(area) for the Bobcat site (−0.74) was more negative than the log(area) slope for all sites (−0.21), indicating the sediment delivery rates decreased more steeply across the range of contributing areas at this site as compared to all sites combined (Table IV). In contrast, the log(area) slope for the

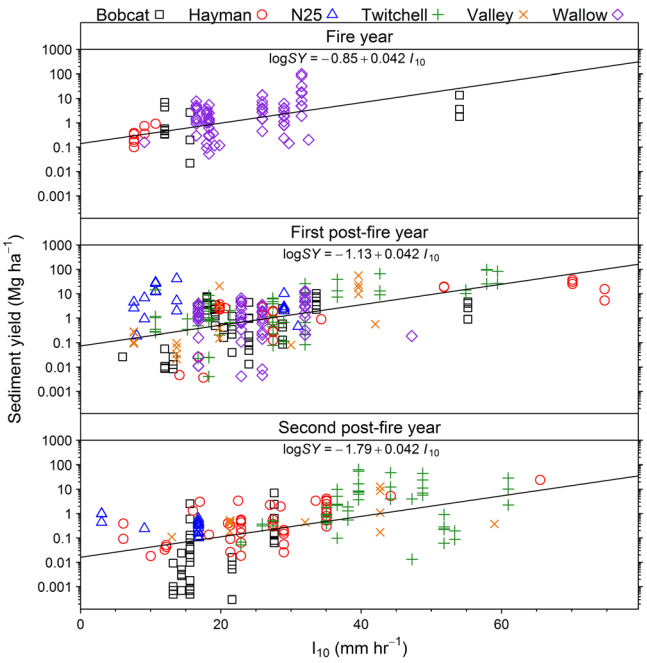

Figure 4. Event sediment yield (*SY*) versus I_{10} by post-fire year. Lines and equations were derived from model coefficients (Table IV) and average values for log(area) and ground cover by year. This figure is available in colour online at wileyonlinelibrary.com/journal/espl

Hayman site (0.076) was greater than the slope for the combined sites (−0.21) (Table IV). More importantly, this term was not significantly different than zero, which indicates the unit-area sediment yields did not vary within the range of contributing areas at the Hayman site. The log(area) slope terms for the other four sites were no different than the slope for the combined model (Table IV).

The ground cover slopes at Hayman (0.00045) and Twitchell (0.0074) were larger than the value for the combined sites (−0.018) and both of the confidence intervals included zero. The Twitchell site, and to a lesser degree the Hayman site, had very high sediment yields in some of the plots with relatively high ground cover. This is especially evident in the Twitchell site in the second post-fire year when high intensity rain events (I_{10} up to 61 mm hr^{-1}) produced large sediment yields (up to 63 Mg ha^{-1}) (Figures 3 and 4). Although it was not different from the slope term for all sites combined, the Valley site had a relatively steep negative ground cover slope (−0.045), which was mainly driven by relatively low ground cover and a broad range in sediment yields in the first post-fire year.

Five of the six sites had modeled slopes for I_{10} that were between 0.036 and 0.054. The one exception (North 25 site, −0.014) was significantly less than the value for the combined-sites (0.042) (Table IV). The negative I_{10} slope term with a wide confidence interval at North 25 was related to two relatively large sediment yields (averaging 16 to 20 Mg ha^{-1} in affected plots) associated with two relatively low intensity rain events (I_{10} values of 11 to 13 mm hr^{-1}) in the first post-fire year (Robichaud *et al.*, 2006).

Contributing area and rainfall intensity as controls on sediment yields

Based on the *F*-values in the all-sites statistical model, the I_{10} was the most significant predictor of sediment yield (F = 228), followed by ground cover (F = 44), log-transformed contributing area (F = 36), and post-fire year (F = 18). When the sediment yield data were separated by the contributing area classes, there were positive relationships between sediment yield and I_{10} across all area classes, and the slopes were significantly greater than zero for all but the largest area class (>10 ha) (Figure 5). The largest area class had the lowest unit-area sediment yields, and the sediment yield–I_{10} slope for this class (0.016) was lower than the slopes for the two middle classes (0.044 and 0.052) although it was not significantly different than the slope for the smallest area class (0.031) because of the small number of observations in the largest area class.

Post-fire sediment delivery ratios (*SDR*s)

The event-based *SDR*s in the sites with nested plots (North 25, Twitchell, and Wallow) ranged from to 0.0003 to 4.0 for the 125 plot-events with non-zero data at multiple scales (Figure 6). The *SDR* declined as both the length ratio and the area ratio between plots increased, but the length ratio was a more significant factor (F = 41) than the log-transformed area ratio (F = 14). This means that as the length ratio and therefore the distance downstream increased, the amount of sediment delivered decreased. The equation for the relationship between post-SDR and length ratio was

$$\log(\text{SDR}) = -0.66 - 0.0074(\text{length ratio}) \qquad (3)$$

The $R^2_{\text{LMM(cov)}}$ for the log-transformed *SDR*, which included the random factor (repeated measures on plots within sites) and the length ratio, was 0.25.

The annual *SDR*s (Figure 7) had a smaller range (0.0089 to 1.15) than the event-based ratios (Figure 6). The modeled line between the annual *SDR* and length ratio was similar to that of the event-based *SDR* except that the slope was steeper in the annual model (Figure 7). The $R^2_{\text{LMM(cov)}}$ for the annual sediment delivery model was 0.74, but we recognize this relatively high fraction of accounted-for variability was based on few data over a large range of length ratios.

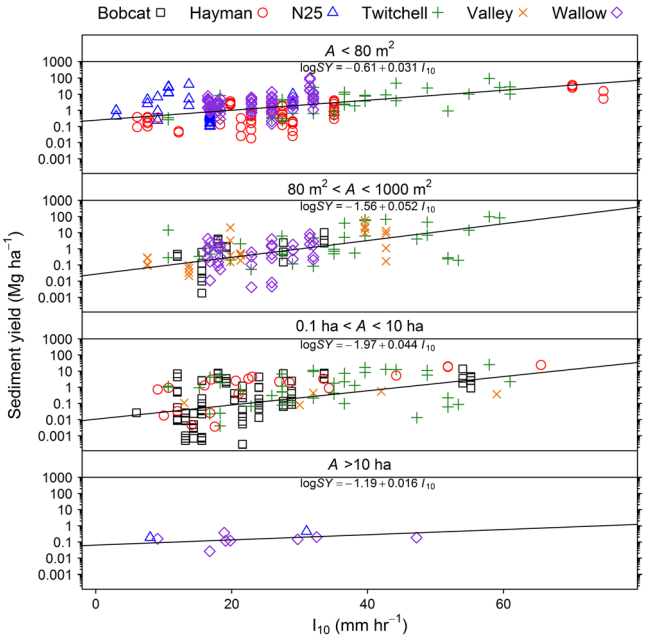

Figure 5. Event sediment yield (*SY*) versus I_{10} by area (*A*) class. Lines and equations were derived from model coefficients and average ground cover values for each area class. This figure is available in colour online at wileyonlinelibrary.com/journal/espl

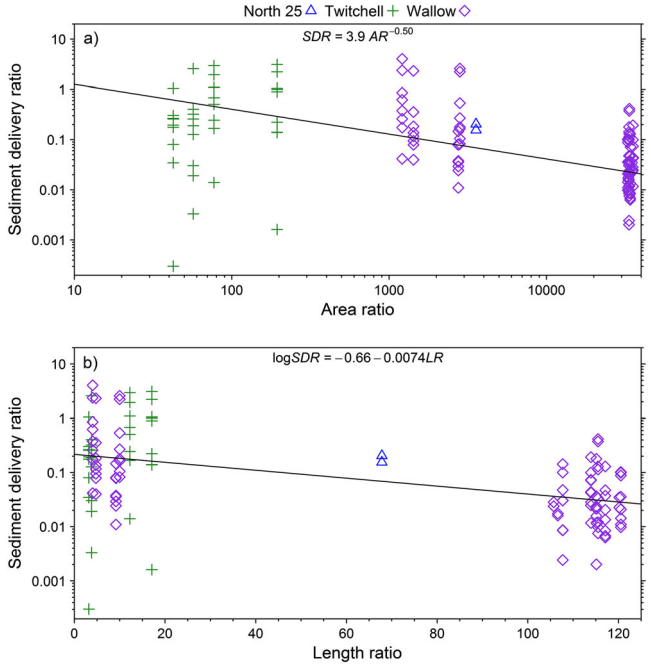

Figure 6. Sediment delivery ratio (*SDR*) versus (a) area ratio (*AR*) and (b) length ratio (*LR*) for the three sites with nested plots (North 25, Twitchell, and Wallow). All ratios are the catchment value divided by the plot value. Lines and equations were derived from model coefficients. Total number of plot-events is 125 (North 25: 2; Twitchell: 35; Wallow: 88). This figure is available in colour online at wileyonlinelibrary.com/journal/espl

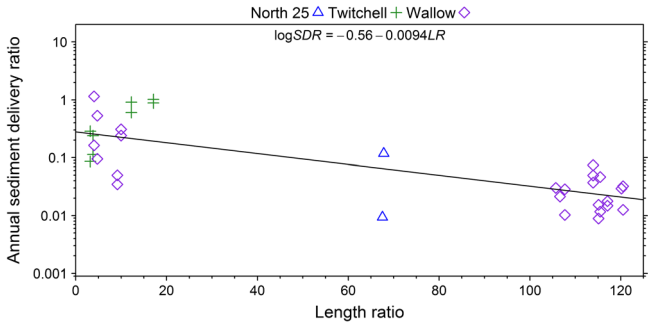

Figure 7. Annual sediment delivery ratio (*SDR*) versus length ratio (*LR*) for the three sites with nested plots (North 25, Twitchell, and Wallow). Both ratios are the catchment value divided by the plot value. Line and equation were derived from model coefficients. Total number of plot-years is 34 (North 25: 2; Twitchell: 8; Wallow: 24). This figure is available in colour online at wileyonlinelibrary.com/journal/espl

Discussion

Spatial scales and processes

The contributing area, time since burning, and rainfall intensity are three scalar controls on post-fire sediment yields. The area above a point in the hillslope or catchment controlled the sediment delivery at that point under given rainfall and post-fire conditions, as described by Equation 1. The downstream reduction in sediment delivery was also affected by the plot lengths – which were correlated to the area of the plots because of the small range in the width of the nested plots – with significantly less sediment delivery as the catchment length increased relative to the plot length (Figure 6). Assuming constant variability in infiltration, roughness properties, and microrelief, the flow path length controls the likelihood of the runoff infiltrating, encountering increased resistance to flow, or being held in detention storage, and thereby controls the connectivity of runoff (Bracken and Croke, 2007; Gomi *et al.*, 2008; Mayor *et al.*, 2008; Reaney *et al.*, 2013) and the resultant ability of the runoff to transport sediment.

The spatial scales addressed in the current study (20 m^2 – 117 ha) comprise several major processes of fluvial sediment transport. Many of these individual processes have been quantified in unburned landscapes, and to a lesser degree, in burned landscapes. Rainsplash is a dominant process at scales on the order of a meter (Planchon and Mouche, 2010), but the soil detached during rainsplash is an important sediment source for sediment delivery at larger spatial scales, including sheetwash (Young and Wiersma, 1973; Morgan, 1978; Fox and Bryan, 1999), and rilling (Asadi *et al.*, 2007; Robichaud *et al.*, 2010; McGuire *et al.*, 2013). Rainsplash also increases sealing on bare soil (Bradford *et al.*, 1987; Bryan, 2000; Larsen *et al.*, 2009), thereby increasing runoff and providing a positive erosion feedback because of the deeper flow if no protective crust forms. Sheetwash dominates sediment transport on non-convergent slopes (Montgomery and Dietrich, 1994) but it produces less erosion than rainsplash at finer scales or rilling at larger scales (Bryan, 2000).

Rills were observed in some of the smallest hillslope plots and in many of the larger hillslope plots and catchments in the current study. Rilling is the dominant hillslope erosion mechanism in burned areas in the western United States (Moody and Martin, 2001a; Moody and Kinner, 2006; Pietraszek, 2006; Larsen *et al.*, 2009; Robichaud *et al.*, 2010) and in a study using unburned plots in Arizona, the apparent increase in sediment delivery with increasing area at the hillslope scale was attributed to rill erosion (Parsons *et al.*, 2006a). Hillslope surface roughness partly controls the resultant rill pattern (Favis-Mortlock *et al.*, 2000), and smoother slopes that are commonly found in recently burned areas would tend to have parallel rather than dendritic drainage patterns (McGuire *et al.*, 2013) and therefore shorter flow paths, steeper gradients, increased energy for erosion and sediment transport, and increased sediment delivery potential.

Small gullies or channel head cuts were also observed at some of the sites. Gullies can be a significant source of sediment in burned areas (Istanbulluoglu *et al.*, 2002) as well as an efficient pathway for post-fire sediment transport (Blake *et al.*, 2009). de Vente and Poesen (2005) suggest a critical-area threshold for gully formation in unburned areas of 3 ha, whereas reports from burned areas suggest this threshold might be on the order of 0.1 to 0.2 ha (Moody and Kinner, 2006). Gully assessments in burned areas indicate the degree of burn severity and rainfall intensity are important factors for reactivation of gullies (Hyde *et al.*, 2007) and that rilling may lead to debris flows and leave deep gullies in burned areas (Gabet and Bookter, 2008; Santi *et al.*, 2008).

Channel erosion and sediment transport and deposition are the dominant sediment delivery processes at larger spatial scales (de Vente and Poesen, 2005). At the largest scales in our study, we observed channel processes including incision and bank erosion, deposition in point bars and associated with woody debris jams, and energy dissipation associated with roughness elements including boulders, tree roots, and channel steps. Rapid, large-scale channel incision via flood or debris flows commonly cited in the post-fire literature (Meyer and Wells, 1997; Cannon and Reneau, 2000; Cannon *et al.*, 2001a, 2001b; Benda *et al.*, 2003; Legleiter *et al.*, 2003; Shakesby and Doerr, 2006; Gabet and Bookter, 2008; Santi *et al.*, 2008) did not occur uniformly at any of the six study sites, but there were several instances of local channel scour.

The slope for the log-transformed area in the sediment yield model for the Bobcat site was more negative (−0.74) than the corresponding slope for all sites (−0.21), indicating the sediment delivery rates decreased more steeply across the range

of contributing areas at this site as compared to all sites combined. This may have been due to the exclusion of channel processes in the erosion and sediment transport in the larger, unchanneled plots at this site (Table III).

Effect of time on post-fire sediment delivery

Our event-based *SDR*s spanned at least two orders of magnitude at the Twitchell and Wallow sites (Figure 6). The annual *SDR*s were less variable, indicating the importance of the selected timescale in the accounting for the sediment delivery rates (Keller *et al.*, 1997; Moody and Martin, 2001a). This result also demonstrates the variability in post-fire delivery ratios and their dependence on site conditions including vegetation, flow path length, rainfall intensity, and factors not explicitly measured here such as runoff rate and duration, channel confinement and geologic parent material. At the Wallow site we observed sediment delivery at the catchment scale from snowmelt runoff with no corresponding hillslope sediment delivery. This demonstrates the need for sufficient runoff to produce sediment transport in larger catchments and the runoff that produces in-channel transport may be temporally disconnected from the processes of erosion at the hillslope scale (Walling, 1983). The delivery at the catchment scale without hillslope erosion also indicates potential differences in process-specific connectivity across spatial scales within a burned catchment. The temporal disconnect related to the sediment transport from snowmelt in the current study was on the order of six or seven months, but several of the event-based *SDR*s were greater than one (Figure 6), indicating temporal disconnects on the timescale of individual events. A few other studies have addressed the potential timescale of post-fire sediment delivery, and these have estimated that sediment delivered to main stem channels may remain there for years (Kunze and Stednick, 2006; Reneau *et al.*, 2007), decades (Heede *et al.*, 1988; Mayor *et al.*, 2007), or longer (Meyer *et al.*, 1992; Moody and Martin, 2001a).

The time since burning (post-fire year), which has been shown to be a control on sediment yields in earlier studies (Helvey, 1980; Morris and Moses, 1987; Cerdà and Doerr, 2005; Wagenbrenner *et al.*, 2006; Mayor *et al.*, 2007; Pierson *et al.*, 2008; Robichaud *et al.*, 2008b, 2013b, 2013c), is an indirect measure of vegetative and hydrologic recovery. Ground cover increases at different rates across different ecosystems, and this can be seen by the relatively broad range of cover values over the two post-fire years (Figure 3). Increases in vegetation and litter cover in later post-fire years (e.g. Figure 3) directly reduce raindrop impact on the soil surface, and thereby lead to lower rates of splash erosion (Planchon and Mouche, 2010). Reduced raindrop impact also results in higher infiltration and lower overland flow rates (Johansen *et al.*, 2001; Cerdà and Doerr, 2005; Pierson *et al.*, 2009). Ground cover also increases surface roughness and so may increase the flow path length (McGuire *et al.*, 2013) and reduce runoff velocity and sediment transport capacity (Robichaud *et al.*, 2010; Wagenbrenner *et al.*, 2010; Robichaud *et al.*, 2013a). The sediment supply on hillslopes may become source limited as sediment-producing events occur (Smith and Dragovich, 2008), and this may lead to lower sediment yields with the occurrence of subsequent erosional events.

Effect of rainfall intensity on sediment delivery

The third scalar control on sediment delivery, rainfall intensity, indirectly measures the amount of energy conveyed by rainfall to the soil surface, and thereby controls rain splash erosion rates (Young and Wiersma, 1973; Dunkerley, 2008). Rainfall intensity also affects the amount of surface runoff that is generated via infiltration excess overland flow and the amount of rill erosion on hillslopes (Berger *et al.*, 2010) as well as peak discharge rates (Moody and Martin, 2001b) and suspended sediment loads (Kunze and Stednick, 2006) in burned areas. The sediment-producing events were almost all very local, high-intensity, convective storms. In our analysis of the sediment yield–I_{10} relationship across area classes (Figure 5) the largest area class had the lowest slope. The lower slope suggests the rainfall intensity was less of a control on sediment yields at the largest (> 10 ha) scale, and this may be related to the small spatial extent of the convective storms relative to the burned catchments. The variability of fire effects on soil properties also increases at larger scales (e.g. Woods *et al.*, 2007) and this would result in a greater likelihood of the runoff infiltrating or being detained in a lower-severity burned area, thereby reducing the sediment delivery rate in the larger spatial scales.

Other considerations

The spatial extent of the rain storm relative to the burned area of interest influences the connectivity of post-fire runoff and sediment delivery. The severity and size of burned patches affect the amount of runoff and sediment generated (Turner *et al.*, 1994; DeBano *et al.*, 1998; Benavides-Solorio and MacDonald, 2001, 2005; Moody *et al.*, 2008b; Robichaud *et al.*, 2010), and the severity, size, and spatial arrangement of burned patches control the downstream transport of runoff and sediment (Bracken and Croke, 2007; Mayor *et al.*, 2011). The spatial extent of rain storms interacts with the patch size and connectivity of burned areas to control the amount of runoff and sediment delivery. Surface runoff generated by intense rainstorms that are smaller than the burned patch (or catchment) may infiltrate into the soil downstream of the storm or patch, resulting in low sediment delivery rates. Conversely, surface runoff generated by intense rainstorms that are larger than the burned patch (or catchment) will be less likely to infiltrate downstream and will therefore increase sediment delivery rates.

The Hayman site appears unique among these six sites in that the sediment yields did not decline with increasing contributing area (Table IV) and that little reduction in sediment yield occurred over the first two post-fire years. The underlying geology varied among the six sites (Table I) but the Pike's Peak granite at the Hayman site weathers to grüs (Moody and Kinner, 2006). This gravelly soil has relatively high infiltration rates in unburned conditions (Graham, 2003) but has low vegetative recovery rates (Robichaud *et al.*, 2013b) and can produce high runoff rates and become very mobile in post-fire conditions (Moody and Martin, 2001a; Robichaud *et al.*, 2013c). The highly mobile soil may have contributed to greater rill erosion rates in the catchments at this site compared to the other sites and thereby produced the lack of a relationship between contributing area and sediment yields (de Vente *et al.*, 2007; Robichaud *et al.*, 2013c).

The Hayman results demonstrate that the post-fire sediment delivery rates across scales will depend on specific site factors such as soil properties or parent material and other hydrologic characteristics as they do in unburned catchments (Walling, 1983; de Vente and Poesen, 2005; Lu *et al.*, 2005). Other limitations on the use of the *SDR*, especially the lack of specific description of the erosion, transport, and deposition processes, have been well described (Walling, 1983; Parsons *et al.*, 2006b). However, despite

the lack of accounting for processes in the *SDR*, this approach can be used to estimate the downstream sediment delivery rates from coarse soils affected by high severity fires using values measured in small monitoring plots or predicted by hillslope erosion models.

We recognize that because of the differences in soils, topography, vegetation, and climate among sites that no single statistically-based sediment delivery equation would be applicable to all burned areas throughout the western United States, let alone in other regions around the world. At the same time, the similarity of the coefficients in the statistical equations for five of the six sites suggest that these equations may be suitable as a first approximation for extrapolating post-fire sediment delivery rates at larger scales (e.g. on the order of 1 km^2) from measured or modeled values derived for smaller plots in the interior western United States. Development of similar statistical equations for fire-prone regions with different hydro-geomorphic responses (Moody *et al.*, 2013), such as in southern California, the Mediterranean basin, and Australia, would be an important scientific contribution.

Future research should address physical processes so that we can better understand and physically model downstream post-fire sediment delivery. There are several immediate research needs including: better identification of post-fire sediment sources, possibly using tracer methods (Blake *et al.*, 2009; Smith *et al.*, 2013); defining the key physical controls on sediment delivery in burned catchments; establishing explicit rainfall–runoff responses for burned areas (Moody and Martin, 2001b; Moody *et al.*, 2008b, 2013); addressing the temporal and spatial connectivity in post-fire runoff given the patchiness of burned areas (Doerr and Moody, 2004; Moody *et al.*, 2013) and different runoff processes; and describing the changes of these processes and controls over time through the post-fire recovery period.

Conclusions

Six sites with plot and catchment measurements were used to develop statistical relationships between post-fire bedload sediment yields, rainfall, and site characteristics. The contributing areas ranged from 20 m^2 to 117 ha. The sediment yields significantly decreased with increasing contributing area at all but one site. The sediment yields also were positively related to rainfall intensity and negatively related to ground cover, as has been shown in previous studies. The *SDR*s in the catchments with nested plots decreased significantly as the difference in size between the plot and catchment increased and the ratio of lengths more significantly affected the delivery ratio than the ratio of areas. A statistical equation relating sediment yields to controlling site factors (log-transformed contributing area, post-fire year, and ground cover) and rainfall intensity and a second equation relating *SDR* to length ratio were developed from the measured data. These results will help constrain estimates of catchment-scale post-fire sediment delivery rates developed from hillslope measurements or models.

Acknowledgements—This work was supported in part by a National Needs Fellowship grant from the US Department of Agriculture, National Institute of Foods and Agriculture, under agreement no. 2008-38420-04761. Additional funding was provided by the US Department of Agriculture, Forest Service through the Rocky Mountain Research Station and the Pike-San Isabel, Apache-Sitgreaves, and Fishlake National Forests. The authors thank the employees from the above Forest Service offices as well as the Arapahoe-Roosevelt, Bitterroot, and Okanagan-Wenatchee National Forests for their assistance in data collection and processing. The authors appreciate early discussions with Lee MacDonald, Isaac Larsen, and Peter Nelson that helped focus this study, and also thank the associate editor and two anonymous reviewers for their comments.

References

Arkell RE, Richards F. 1986. Short duration rainfall relations for the western United States. In Proceedings of the Conference on Climate and Water Management-A Critical Era and Conference on the Human Consequences of 1985s Climate. American Meteorological Society: Boston, MA; 136–141.

Asadi H, Ghadiri H, Rose CW, Rouhipour H. 2007. Interrill soil erosion processes and their interaction on low slopes. *Earth Surface Processes and Landforms* **32**: 711–724. DOI: 10.1002/esp.1426

Benavides-Solorio JD, MacDonald LH. 2001. Post-fire runoff and erosion from simulated rainfall on small plots, Colorado Front Range. *Hydrological Processes* **15**: 2931–2952. DOI: 10.1002/hyp.383

Benavides-Solorio JD, MacDonald LH. 2005. Measurement and prediction of post-fire erosion at the hillslope scale, Colorado Front Range. *International Journal of Wildland Fire* **14**: 457–474. DOI: 10.1071/WF05042

Benda LE, Miller D, Bigelow P, Andras K. 2003. Effects of post-wildfire erosion on channel environments, Boise River, Idaho. *Forest Ecology and Management* **178**: 105–119.

Berger C, Schulze M, Rieke-Zapp DH, Schlunegger F. 2010. Rill development and soil erosion: a laboratory study of slope and rainfall intensity. *Earth Surface Processes and Landforms* **35**: 1456–1467. DOI: 10.1002/esp.1989

Blake WH, Wallbrink PJ, Wilkinson SN, Humphreys GS, Doerr SH, Shakesby RA, Tomkins KM. 2009. Deriving hillslope sediment budgets in wildfire-affected forests using fallout radionuclide tracers. *Geomorphology* **104**: 105–116.

Bonnin GM, Martin DA, Lin B, Parzybok T, Yekta M, Riley D. 2004. NOAA Atlas 14: Precipitation-Frequency Atlas of the United States, Volume 1, Version 5, Semiarid Southwest (Arizona, Southeast California, Nevada, New Mexico, Utah). National Oceanic and Atmospheric Administration (NOAA): Silver Spring, MD.

Bracken LJ, Croke J. 2007. The concept of hydrological connectivity and its contribution to understanding runoff-dominated geomorphic systems. *Hydrological Processes* **21**: 1749–1763. DOI: 10.1002/hyp.6313

Bradford JM, Ferris JE, Remley PA. 1987. Interrill soil erosion processes: I. Effect of surface sealing. *Soil Science Society of America Journal* **51**: 1566–1571.

Brown JAH. 1972. Hydrologic effects of a bushfire in a catchment in south-eastern New South Wales. *Journal of Hydrology* **15**: 77–96.

Bryan RB. 2000. Soil erodibility and processes of water erosion on hillslope. *Geomorphology* **32**: 385–415.

Cannon SH, Reneau SL. 2000. Conditions for generation of fire-related debris flows, Capulin Canyon, New Mexico. *Earth Surface Processes and Landforms* **25**: 1103–1121.

Cannon SH, Bigio ER, Mine E. 2001a. A process for fire-related debris flow initiation, Cerro Grande fire, New Mexico. *Hydrological Processes* **15**: 3011–3023. DOI: 10.1002/hyp.388

Cannon SH, Kirkham RM, Parise M. 2001b. Wildfire-related debris-flow initiation processes, Storm King Mountain, Colorado. *Geomorphology* **39**: 171–188.

Cerdà A, Doerr SH. 2005. The influence of vegetation recovery on soil hydrology and erodibility following fire: an eleven-year investigation. *International Journal of Wildland Fire* **14**: 1–24.

DeBano LF, Neary DG, Ffolliott PF. 1998. Fire's Effects on Ecosystems. Wiley: New York.

Desilets SLE, Nijssen B, Ekwurzel B, Ferré TPA. 2007. Post-wildfire changes in suspended sediment rating curves: Sabino Canyon, Arizona. *Hydrological Processes* **21**: 1413–1423. DOI: 10.1002/hyp.6352

Doerr SH, Moody JA. 2004. Hydrological effects of soil water repellency: on spatial and temporal uncertainties. *Hydrological Processes* **18**: 829–832. DOI: 10.1002/hyp.5518

Doerr SH, Shakesby RA, Blake WH, Chafer CJ, Humphreys GS, Wallbrink PJ. 2006. Effects of differing wildfire severities on soil wettability and implications for hydrological response. *Journal of Hydrology* **319**: 295–311.

Dunkerley D 2008. Rain event properties in nature and in rainfall simulation experiments: a comparative review with recommendations for increasingly systematic study and reporting. *Hydrological Processes* **22**: 4415–4435. DOI: 10.1002/hyp.7045

Ebel BA, Moody JA, Martin DA. 2012. Hydrologic conditions controlling runoff generation immediately after wildfire. *Water Resources Research* **48**: W03529. DOI: 10.1029/2011WR011470

Favis-Mortlock DT, Boardman J, Parsons AJ, Lascelles B. 2000. Emergence and erosion: a model for rill initiation and development. *Hydrological Processes* **14**: 2173–2205.

Ferreira AJD, Coelho C de OA, Ritsema CJ, Boulet A-K, Keizer JJ. 2008. Soil and water degradation processes in burned areas: lessons learned from a nested approach. *Catena* **74**: 273–285. DOI: 10.1016/j.catena.2008.05.007

Fox DM, Bryan RB. 1999. The relationship of soil loss by interrill erosion to slope gradient. *Catena* **38**: 211–222.

Gabet EJ, Bookter A. 2008. A morphometric analysis of gullies scoured by post-fire progressively bulked debris flows in southwest Montana, USA. *Geomorphology* **96**: 298–309.

Gomi T, Sidle RC, Miyata S, Kosugi K, Onda Y. 2008. Dynamic runoff connectivity of overland flow on steep forested hillslopes: scale effects and runoff transfer. *Water Resources Research* **44**: W08411. DOI: 10.1029/2007WR005894

Graham RT (ed.). 2003. Hayman Fire Case Study, General Technical Report RMRS-GTR-114. US Department of Agriculture, Forest Service, Rocky Mountain Research Station: Fort Collins, CO.

Haire SL, McGarigal K. 2010. Effects of landscape patterns of fire severity on regenerating ponderosa pine forests (Pinus ponderosa) in New Mexico and Arizona, USA. *Landscape Ecology* **25**: 1055–1069. DOI: 10.1007/s10980-010-9480-3.

Heede BH. 1985. Channel adjustments to the removal of log steps: an experiment in a mountain stream. *Environmental Management* **9**: 427–432.

Heede BH, Harvey MD, Laird JR. 1988. Sediment delivery linkages in a chaparral watershed following a wildfire. *Environmental Management* **12**: 349–358. DOI: 10.1007/BF01867524

Helvey JD. 1980. Effects of a north central Washington wildfire on runoff and sediment production. *Journal of the American Water Resources Association* **16**: 627–634. DOI: 10.1111/j.1752-1688.1980.tb02441.x

Hyde KD, Woods SW, Donahue J. 2007. Predicting gully rejuvenation after wildfire using remotely sensed burn severity data. *Geomorphology* **86**: 496–511. DOI: 10.1016/j.geomorph.2006.10.012

Istanbulluoglu E, Tarboton DG, Pack RT, Luce CH. 2002. A probabilistic approach for channel initiation. *Water Resources Research* **38**: 1325. DOI: 10.1029/2001wr000782

Johansen MP, Hakonson TE, Breshears DD. 2001. Post-fire runoff and erosion from rainfall simulation: contrasting forests with shrublands and grasslands. *Hydrological Processes* **15**: 2953–2965. DOI: 10.1002/hyp.384

Keeley JE. 2009. Fire intensity, fire severity and burn severity: a brief review and suggested usage. *International Journal of Wildland Fire* **18**: 116–126. DOI: 10.1071/WF07049

Keller EA, Valentine DW, Gibbs DR. 1997. Hydrological response of small watersheds following the southern California Painted Cave fire of June 1990. *Hydrological Processes* **11**: 401–414.

Kunze MD, Stednick JD. 2006. Streamflow and suspended sediment yield following the 2000 Bobcat fire, Colorado. *Hydrological Processes* **20**: 1661–1681. DOI: 10.1002/hyp.5954

Lane PNJ, Sheridan GJ, Noske PJ. 2006. Changes in sediment loads and discharge from small mountain catchments following wildfire in south eastern Australia. *Journal of Hydrology* **331**: 495–510.

Lanini JS, Clark EA, Lettenmaier DP. 2009. Effects of fire-precipitation timing and regime on post-fire sediment delivery in Pacific Northwest forests. *Geophysical Research Letters* **36**: L01402. DOI: 10.1029/2008gl034588

Larsen IJ, MacDonald LH, Brown E, Rough D, Welsh MJ, Pietraszek JH, Libohova Z, Benavides-Solorio JD, Schaffrath K. 2009. Causes of post-fire runoff and erosion; water repellency, cover, or soil sealing? *Soil Science Society of America Journal* **73**: 1393–1407. DOI: 10.2136/sssaj2007.0432

Legleiter CJ, Lawrence RL, Fonstad MA, Marcus WA, Aspinall R. 2003. Fluvial response a decade after wildfire in the northern Yellowstone ecosystem: A spatially explicit analysis. *Geomorphology* **54**: 119–136.

Littell RC, Milliken G, Stroup W, Wolfinger R, Schabenberger O. 2006. SAS for Mixed Models, 2nd edn. SAS Institute, Inc.: Cary, NC.

Lu H, Moran CJ, Sivapalan M. 2005. A theoretical exploration of catchment-scale sediment delivery. *Water Resources Research* **41**: W09415. DOI: 10.1029/2005WR004018

Malmon DV, Reneau SL, Katzman D, Lavine A, Lyman J 2007. Suspended sediment transport in an ephemeral stream following wildfire. *Journal of Geophysical Research* **112**: F02006. DOI: 10.1029/2005jf000459

Martin DA, Moody JA. 2001. Comparison of soil infiltration rates in burned and unburned mountainous watersheds. *Hydrological Processes* **15**: 2893–2903. DOI: 10.1002/hyp.380

Mayor ÁG, Bautista S, Llovet J, Bellot J. 2007. Post-fire hydrological and erosional responses of a Mediterranean landscape: seven years of catchment-scale dynamics. *Catena* **71**: 68–75.

Mayor ÁG, Bautista S, Small EE, Dixon M, Bellot J. 2008. Measurement of the connectivity of runoff source areas as determined by vegetation pattern and topography: a tool for assessing potential water and soil losses in drylands. *Water Resources Research* **44**: W10423. DOI: 10.1029/2007WR006367

Mayor ÁG, Bautista S, Bellot J. 2011. Scale-dependent variation in runoff and sediment yield in a semiarid Mediterranean catchment. *Journal of Hydrology* **397**: 128–135. DOI: 10.1016/j.jhydrol.2010.11.039

McGuire LA, Pelletier JD, Gómez JA, Nearing MA. 2013. Controls on the spacing and geometry of rill networks on hillslopes: Rain splash detachment, initial hillslope roughness, and the competition between fluvial and colluvial transport. *Journal of Geophysical Research: Earth Surface* **118**: 241–256. DOI: 10.1002/jgrf.20028

Meyer GA, Wells SG. 1997. Fire-related sedimentation events on alluvial fans, Yellowstone National Park, U.S.A. *Journal of Sedimentary Research* **67**: 776–791. DOI: 10.1306/d426863a-2b26-11d7-8648000102c1865d

Meyer GA, Wells SG, Balling Jr RC, Jull AJT. 1992. Response of alluvial systems to fire and climate change in Yellowstone National Park. *Nature* **357**: 147–150.

Miller JF, Frederick RH, Tracey RJ. 1973. NOAA Atlas 2: Precipitation-Frequency Atlas of the Western United States. National Oceanic and Atmospheric Administration (NOAA): Silver Spring, MD.

Montgomery DR, Dietrich WE. 1994. Landscape dissection and drainage area-slope thresholds. In Process Models and Theoretical Geomorphology, Kirkby MJ (ed.). John Wiley & Sons: Chichester; 221–246.

Moody JA, Kinner DA. 2006. Spatial structures of stream and hillslope drainage networks following gully erosion after wildfire. *Earth Surface Processes and Landforms* **31**: 319–337. DOI: 10.1002/esp.1246

Moody JA, Martin DA. 2001a. Initial hydrologic and geomorphic response following a wildfire in the Colorado Front Range. *Earth Surface Processes and Landforms* **26**: 1049–1070. DOI: 10.1002/esp.253

Moody JA, Martin DA. 2001b. Post-fire, rainfall intensity-peak discharge relations for three mountainous watersheds in the western USA. *Hydrological Processes* **15**: 2981–2993. DOI: 10.1002/hyp.386

Moody JA, Martin DA. 2009. Synthesis of sediment yields after wildland fire in different rainfall regimes in the western United States. *International Journal of Wildland Fire* **18**: 96–115. DOI: 10.1071/WF07162

Moody JA, Martin DA, Cannon SH. 2008a. Post-wildfire erosion response in two geologic terrains in the western USA. *Geomorphology* **95**: 103–118.

Moody JA, Martin DA, Haire SL, Kinner DA. 2008b. Linking runoff response to burn severity after a wildfire. *Hydrological Processes* **22**: 2063–2074. DOI: 10.1002/hyp.6806

Moody JA, Shakesby RA, Robichaud PR, Cannon SH, Martin DA. 2013. Current research issues related to post-wildfire runoff and erosion processes. *Earth-Science Reviews* **122**: 10–37. DOI: 10.1016/j.earscirev.2013.03.004

Morgan RPC. 1978. Field studies of rainsplash erosion. *Earth Surface Processes* **3**: 295–299.

Morris SE, Moses TA. 1987. Forest fire and the natural soil erosion regime in the Colorado Front Range. *Annals of the Association of American Geographers* **77**: 245–254.

Nakagawa S, Schielzeth H. 2013. A general and simple method for obtaining R2 from generalized linear mixed-effects models. *Methods in Ecology and Evolution* **4**: 133–142. DOI: 10.1111/j.2041-210x.2012.00261.x

Noske PJ, Lane PNJ, Sheridan GJ. 2010. Stream exports of coarse matter and phosphorus following wildfire in NE Victoria, Australia. *Hydrological Processes* **24**: 1514–1529. DOI: 10.1002/hyp.7616

Ott RL. 1993. An Introduction to Statistical Methods and Data Analysis, 4th edn. Wadsworth Publishing Co.: Belmont, CA.

Parsons AJ, Brazier RE, Wainwright J, Powell DM. 2006a. Scale relationships in hillslope runoff and erosion. *Earth Surface Processes and Landforms* **31**: 1384–1393. DOI: 10.1002/esp.1345

Parsons AJ, Wainwright J, Brazier RE, Powell DM. 2006b. Is sediment delivery a fallacy? *Earth Surface Processes and Landforms* **31**: 1325–1328. DOI: 10.1002/esp.1395

Parsons A, Robichaud PR, Lewis SA, Napper C, Clark JT. 2010. Field Guide for Mapping Post-fire Soil Burn Severity, General Technical Report RMRS-GTR-243. US Department of Agriculture, Forest Service, Rocky Mountain Research Station: Fort Collins, CO.

Pierson FB, Robichaud PR, Moffet CA, Spaeth KE, Hardegree SP, Clark PE, Williams CJ. 2008. Fire effects on rangeland hydrology and erosion in a steep sagebrush-dominated landscape. *Hydrological Processes* **22**: 2916–2929.

Pierson FB, Moffet CA, Williams CJ, Hardegree SP, Clark PE. 2009. Prescribed-fire effects on rill and interrill runoff. *Earth Surface Processes and Landforms* **34**: 193–203. DOI: 10.1002/esp.1703

Pietraszek JH. 2006. Controls on Post-fire Erosion at the Hillslope Scale, Master's Thesis. Colorado State University: Fort Collins, CO; 124 pp.

Planchon O, Mouche E. 2010. A physical model for the action of raindrop erosion on soil microtopography. *Soil Science Society of America Journal* **74**: 1092–1103. DOI: 10.2136/sssaj2009.0063

Prosser IP, Williams L. 1998. The effect of wildfire on runoff and erosion in native Eucalyptus forest. *Hydrological Processes* **12**: 251–265.

Reaney SM, Bracken LJ, Kirkby MJ. 2013. The importance of surface controls on overland flow connectivity in semi-arid environments: results from a numerical experimental approach. *Hydrological Processes* DOI: 10.1002/hyp.9769

Reneau SL, Katzman D, Kuyumjian GA, Lavine A, Malmon DV. 2007. Sediment delivery after a wildfire. *Geology* **35**: 151–154. DOI: 10.1130/g23288a.1

Robichaud PR. 2000. Fire effects on infiltration rates after prescribed fire in Northern Rocky Mountain forests, USA. *Journal of Hydrology* **231-232**: 220–229.

Robichaud PR. 2005. Measurement of post-fire hillslope erosion to evaluate and model rehabilitation treatment effectiveness and recovery. *International Journal of Wildland Fire* **14**: 475–485. DOI: 10.1071/WF05031

Robichaud PR, Brown RE. 2002. Silt Fences: An Economical Technique for Measuring Hillslope Soil Erosion, General Technical Report RM-GTR-94. US Department of Agriculture, Forest Service, Rocky Mountain Research Station: Fort Collins, CO.

Robichaud PR, Lillybridge TR, Wagenbrenner JW. 2006. Effects of postfire seeding and fertilizing on hillslope erosion in north-central Washington, USA. *Catena* **67**: 56–67. DOI: 10.1016/j.catena.2006.03.001

Robichaud PR, Pierson FB, Brown RE, Wagenbrenner JW. 2008a. Measuring effectiveness of three postfire hillslope erosion barrier treatments, western Montana, USA. *Hydrological Processes* **22**: 159–170. DOI: 10.1002/Hyp.6558

Robichaud PR, Wagenbrenner JW, Brown RE, Wohlgemuth PM, Beyers JL. 2008b. Evaluating the effectiveness of contour-felled log erosion barriers as a post-fire runoff and erosion mitigation treatment in the western United States. *International Journal of Wildland Fire* **17**: 255–273. DOI: 10.1071/Wf07032

Robichaud PR, Wagenbrenner JW, Brown RE. 2010. Rill erosion in natural and disturbed forests: 1. Measurements. *Water Resources Research* **46**: W10506. DOI: 10.1029/2009wr008314

Robichaud PR, Jordan P, Lewis SA, Ashmun LE, Covert SA, Brown RE. 2013a. Evaluating the effectiveness of wood shreds and agricultural straw mulches as a treatment to reduce post-fire hillslope erosion in southern British Columbia, Canada. *Geomorphology* **197**: 21–33. DOI: 10.1016/j.geomorph.2013.04.024

Robichaud PR, Lewis SA, Wagenbrenner JW, Ashmun LE, Brown RE. 2013b. Post-fire mulching for runoff and erosion mitigation Part I: Effectiveness at reducing hillslope erosion rates. *Catena* **105**: 75–92. DOI: 10.1016/j.catena.2012.11.015

Robichaud PR, Wagenbrenner JW, Lewis SA, Brown RE, Wohlgemuth PM, Ashmun LE. 2013c. Post-fire mulching for runoff and erosion mitigation Part II: Effectiveness in reducing runoff and sediment yields from small catchments. *Catena* **105**: 93–111. DOI: 10.1016/j.catena.2012.11.016

Rowe PB, Countryman CM, Storey HC. 1954. Hydrologic Analysis used to Determine Effects of Fire on Peak Discharges and Erosion Rates in Southern California Watersheds. US Department of Agriculture, Forest Service, California Forest and Range Experiment Station: Berkeley, CA.

Santi PM, DeWolfe VG, Higgins JD, Cannon SH, Gartner JE. 2008. Sources of debris flow material in burned areas. *Geomorphology* **96**: 310–321.

SAS Institute Inc. 2008. SAS version 9.2. SAS Institute, Inc.: Cary, NC.

Shakesby RA, Doerr SH. 2006. Wildfire as a hydrological and geomorphological agent. *Earth-Science Reviews* **74**: 269–307.

Smith HG, Dragovich D. 2008. Post-fire hillslope erosion response in a sub-alpine environment, south-eastern Australia. *Catena* **73**: 274–285. DOI: 10.1016/j.catena.2007.11.003

Smith HG, Blake WH, Owens PN. 2013. Discriminating fine sediment sources and the application of sediment tracers in burned catchments: A review. *Hydrological Processes* **27**: 943–958. DOI: 10.1002/hyp.9537

Spigel KM, Robichaud PR. 2007. First-year post-fire erosion rates in Bitterroot National Forest, Montana. *Hydrological Processes* **21**: 998–1005. DOI: 10.1002/Hyp.6295

Storrar KAT. 2013. Effectiveness of Straw Bale Check Dams at Reducing Post-fire Sediment Erosion from Ephemeral Channel Catchments, Master's Thesis. University of Montana: Missoula, MT; 103 pp.

Swanson FJ. 1981. Fire and geomorphic processes. In Proceedings of the Conference: Fire Regimes and Ecosystem Properties, General Technical Report WO-GTR-26, Mooney HA, Bonnicksen TM, Christensen NL, Lotan JE, and Reiners WA (eds). US Department of Agriculture, Forest Service: Washington, DC; 401–420.

Troendle CA, Bevenger GS. 1996. Effect of fire on streamflow and sediment transport in Shoshone National Forest, Wyoming. In The Ecological Implications of Fire in Greater Yellowstone, Greenlee JM (ed.). International Association of Wildland Fire: Fairfield, WA; 43–52.

Turner MG, Hargrove WW, Gardner RH, Romme WH. 1994. Effects of fire on landscape heterogeneity in Yellowstone National Park, Wyoming. *Journal of Vegetation Science* **5**: 731–742.

USDA Forest Service. 2011a. Burned Area Report, interim request for the Wallow Fire. US Department of Agriculture, Forest Service: Apache-Sitgreaves National Forest: Springerville, AZ.

USDA Forest Service. 2011b. Wallow Fire Soil Burn Severity Map. US Department of Agriculture, Forest Service: Apache-Sitgreaves National Forest, Springerville, AZ.

Vega JA, Diaz-Fierros F. 1987. Wildfire effects on soil erosion. *Ecologia Mediterranea* **13**: 119–125.

de Vente J, Poesen J. 2005. Predicting soil erosion and sediment yield at the basin scale: Scale issues and semi-quantitative models. *Earth-Science Reviews* **71**: 95–125. DOI: 10.1016/j.earscirev.2005.02.002

de Vente J, Poesen J, Arabkhedri M, Verstraeten G. 2007. The sediment delivery problem revisited. *Progress in Physical Geography* **31**: 155–178. DOI: 10.1177/0309133307076485

Wagenbrenner JW. 2013. Post-fire Stream Channel Processes: Changes in Runoff Rates, Sediment Delivery across Spatial Scales, and Mitigation Effectiveness, Doctoral Dissertation. Washington State University: Pullman, WA; 145 pp.

Wagenbrenner JW, MacDonald LH, Rough D. 2006. Effectiveness of three post-fire rehabilitation treatments in the Colorado Front Range. *Hydrological Processes* **20**: 2989–3006. DOI: 10.1002/Hyp.6146

Wagenbrenner JW, Robichaud PR, Elliot WJ. 2010. Rill erosion in natural and disturbed forests: 2. Modelling approaches. *Water Resources Research* **46**: W10507. DOI: 10.1029/2009wr008315.

Walling DE. 1983. The sediment delivery problem. *Journal of Hydrology* **65**: 209–237.

Wondzell SM, King JG. 2003. Postfire erosional processes in the Pacific Northwest and Rocky Mountain regions. *Forest Ecology and Management* **178**: 75–87.

Woods SW, Birkas A, Ahl R. 2007. Spatial variability of soil hydrophobicity after wildfires in Montana and Colorado. *Geomorphology* **86**: 465–479. DOI: 10.1016/j.geomorph.2006.09.015

Young RA, Wiersma JL. 1973. The role of rainfall impact in soil detachment and transport. *Water Resources Research* **9**: 1629–1636.